Optimization Model of the Transcutaneous Energy Transmission System for Achieving Maximum Power Transfer Capability

Liangyu Bai, Houjun Tang, Yang Xu
Department of Electrical Engineering, School of Electronic, Information and Electrical Engineering,
Shanghai Jiao Tong University, Shanghai, China
Email: liangyubai@gmail.com
{hjtang, xusjtu}@sjtu.edu.cn

***Abstract*—Transcutaneous energy transmission (TET) systems have been a topic of intense research. Such systems play an important role in offering the opportunity to provide power to implantable biomedical devices through wireless power transmission. It eliminates the serious infection risk associated with direct cable connections through the skin. Proper performance of the TET system requires optimization of their electronic component parameters. In this paper, an optimization model is proposed for the preliminary design for two compensated capacitance and two coil inductance. The objective is the power transfer capability of the system. The design variables include the primary and secondary coil inductance. The constrained conditions are peak over-voltage, peak withstand current of the system electronic components and bifurcation phenomenon. This model provides a new and useful tool for determining the compensated capacitance and coil inductance of the TET system. The theoretical analysis is verified by simulated and experimental results. The maximum power transfer capability can be achieved through the optimization solutions in steady-state.**

***Index Terms*—transcutaneous energy transmission (TET) system, power transfer capability, interior point algorithm, biomedical implantable devices**

I. INTRODUCTION

The transcutaneous energy transmission (TET) systems are designed to deliver power from an in vitro primary source to an in vivo implantable device through a dermal skin layer via time-varying electromagnetic fields [1]-[8]. It eliminates the serious risk of infection associated with a direct cable connection through the skin, an advantage recognized decades ago. In the 1960s, John C. Schuder's group from the University of Missouri began to study inductive coupled-radio frequency systems for artificial hearts [2]. For different implanted artificial organ application areas, Guozheng Yan's group from China has performed many experiments on using the TET system for an artificial anal sphincter [3]. Qianhong Chen's group from the Hong Kong Polytechnic University has carried out research into remote energy transfer for an artificial heart [4].

A typical TET system is illustrated in Figure 1. The electromagnetic field generated by the in vitro part of the TET system and produces an induced voltage in the in vivo part of the TET system, then used to charge the biomedical implantable device.

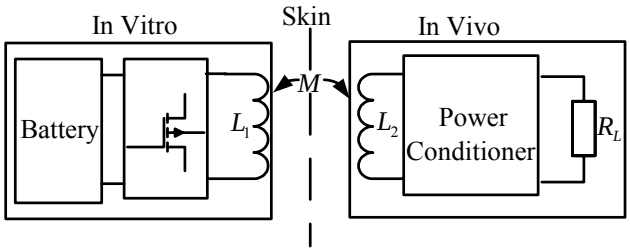

Figure 1. The schematic of the TET system.

Due to a large winding separation, the TET system has relatively large leakage inductance, reduced magnetizing flux, and the mutual coupling is generally weak. Compensation for loose coupling can be achieved through the use of resonance circuits which enable the boosting of voltage or current in the secondary to usable levels. Consequently, the inductance and the capacitance values of the primary and secondary windings need to be optimized to achieve maximum power transfer capability. Therefore, a specific optimization model should be devised for them.

Design optimization of the TET system has been studied extensively. First, several optimization methods have been proposed to increase the power transfer capacity. Wu H. H. has presented an optimal tuning capacitor values to maximize the power transfer capability. The maximum power transfer capacity greater than the traditional method. However, the author did not offer the design method of inductance value [5]. Second, the optimal number of secondary coil winding turns has been proposed in [6] for the highest efficiency under the nominal load and operating frequency; Stanimir Valtchev has proposed a novel method for modeling and analysis of the series loaded series resonant power converters which is a better choice for loosely coupled transformer, and then optimizing it for the best possible efficiency [7].

doi:10.4304/jcp.6.2.305-312

The researchers mentioned above have performed a great deal of work on TET systems that provide power to biomedical implantable devices. Unfortunately, these studies do not include a general method for selecting the optimal matching parameters of inductance and capacitance in the resonant circuits used for achieving maximum power transfer capability.

This study has focused on a general design that determines the optimal matching parameters of capacitance and inductance values for a TET system to achieve maximum power transfer. In order to achieve this goal, the mutual inductance coupling model and its equivalent parameters commonly used in TET system design have been introduced in Section II. In Section III, the optimization model of the TET system is analyzed in detail. In Section IV, the simulation and experimental verification is presented. Finally, conclusions are summarized in Section V.

II. ELECTRICAL MODEL OF THE TET SYSTEM

A. Mutual inductance coupling model

The TET system discussed here transfers power through two independent mutually coupled coils, which are being separated by human skin. The N-MOSFET (Negative-Channel Metal-Oxide- Semiconductor Field-Effect Transistor) H-bridge inverter is chosen as the power driving circuit.

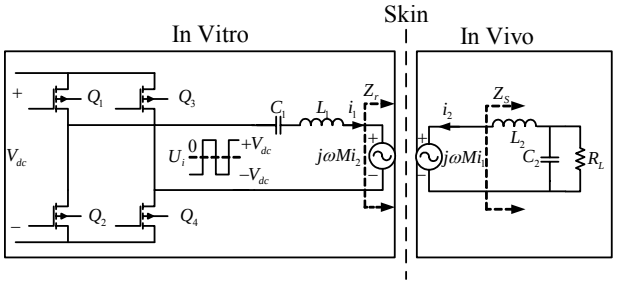

Figure 2. Mutual inductance coupling model of the TET system.

The equivalent mutual inductance coupling circuit model is shown in Figure 2, where V_{dc} is the input DC voltage, Q_1 , Q_2 , Q_3 and Q_4 are power MOSFETs, L_1 and L_2 stand for the primary and secondary coils, C_1 and C_2 are their compensation capacitances, M is the mutual inductance between L_1 and L_2 , and k is coupling coefficient. In order to simplify the optimization model and the algorithm, the equivalent series resistance of the primary capacitance and inductance, the internal resistance of the battery, and the ON resistance of the MOSFETs are neglected. The equivalent series resistance of the secondary capacitance and inductance are also neglected. $j\omega Mi_2$ is the reflected voltage in the external primary part due to the secondary current i_2 , while the induced voltage in the implantable secondary part due to the primary current i_1 is equal to $j\omega Mi_1$. ω is the angular operational frequency. The subscripts 1 and 2 stand for the primary and secondary respectively. The resistance R_L represents the load on the implantable secondary. Similar optimization model can be built for the other three basic topologies, such as Series-Series, Parallel-Parallel, and Parallel-Series. The topology analyses for these alternatives can be found in [9].

Under steady state conditions, the TET system is operating at a constant frequency, constant coupling coefficient and constant load. The circuit parameters are shown in TABLE I.

TABLE I. TET SYSTEM PARAMETERS

Parameters	Value	Parameters	Value
f	40kHz	k	0.24
V_{dc}	15V	R_L	20Ω

B. Power transfer capability

The TET system voltage U_i is supplied by an H-bridge inverter is shown in Figure 2, which is a square wave. The amplitude of the U_i can be considered as a constant. The U_i can be factorized as a Fourier series, and can be derived as:

$$U_i = \frac{4U_{dc}}{\pi}(\sin\omega t + \frac{1}{3}\sin 3\omega t + \frac{1}{5}\sin 5\omega t + \cdots) \quad (1)$$

The RMS (Root-Mean-Square) value of the fundamental component of U_i is:

$$U_1 = \frac{2\sqrt{2}V_{dc}}{\pi} \quad (2)$$

According to the mutual inductance coupling model, the reflected impedance Z_r from the implantable secondary to the external primary is dependent on the mutual inductance M and the angular operational frequency ω , and can be expressed as:

$$Z_r = \frac{\omega^2 M^2}{Z_s} \quad (3)$$

where Z_s is the impedance of the implantable secondary, whose value depends on the secondary compensation circuit as shown in:

$$Z_s = j\omega L_2 + \frac{R_L}{1 + j\omega C_2 R_L} \quad (4)$$

To minimize the VA rating of the power supply and to ensure maximum power transfer capability, the compensated capacitance is calculated [9], as shown in:

$$C_1 = 1/(\omega^2 L_1 - \omega^2 M^2 / L_2) \quad (5)$$

$$C_2 = 1/(\omega^2 L_2) \quad (6)$$

The power transferred from the external primary to the implantable secondary can be defined as:

$$P_2 = I_1^2 \times \mathrm{Re}\, Z_r = (\frac{U_1}{Z_{in}})^2 \times \mathrm{Re}\, Z_r \quad (7)$$

where Z_{in} is the amplitude of the load impedance seen by the power supply.

Substituting (2) into (7), the power transferred from the external primary to the implantable secondary P_2 is determined by:

$$P_2 = \frac{8\,\mathrm{Re}\,Z_r V_{dc}^2}{\pi^2 Z_{in}^2} \tag{8}$$

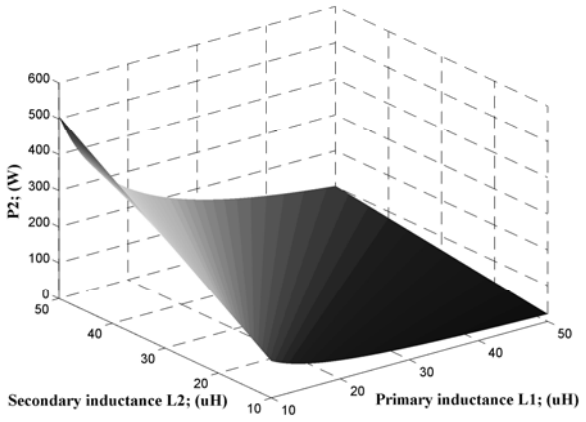

Figure 3. Objective function variation with primary and secondary inductance.

The variation of the transfer power capability in terms of the primary and secondary inductance is shown in Figure 3. It is seen that an increase in the secondary inductance L_2 and a reduction in the primary inductance L_1 can lead to an increase in the power transfer capability.

III. Optimization Model of the TET System

Optimizations would be necessary if we want better performances. In this section, an optimization model will be built for the TET system, including the design variables, the objectives, and the constraints.

Design variables are those parameters that will change during the optimization process. L_1 and L_2 are design variables. The power transfer capability is the objective considered in this model. To obtain an optimal design considering power transfer capability, objective function $P_2(L_1, L_2)$ is proposed where $P_2(L_1, L_2)$ is the function of the power transfer capability. The constraints are divided into two parts:

A. Constrained inequality based on bifurcation phenomenon

When the TET system is optimized, it is desirable to analyze the bifurcation region based on stability consideration [9]. In such a region, the operating frequency will either drift away from the ideal operating point or move in an unstable state. Therefore, we must ensure these proposed optimization parameters operate out of the bifurcation region.

In the series compensated primary and parallel compensated secondary topology, the bifurcation boundary is shown in:

$$Q_1 > Q_2 + \frac{1}{Q_2} \tag{9}$$

where Q_1 , Q_2 are the primary and secondary quality factors.

The bifurcation region can be derived as:

$$L_2 < \frac{kR_L}{\omega_0\sqrt{1-k^2}} = k_a \tag{10}$$

where ω_0 is operating resonant frequency. The secondary inductance L_2 should be chosen out of the bifurcation region, as shown in inequality (10).

When the secondary inductance L_2 is higher than k_a , the system will be operated out of the bifurcation region. To show the influence of the secondary inductance on the bifurcation phenomenon, it can be seen in Figure 4 that how phase angle of the load impedance varies when the secondary inductance increases. k_a (dotted line) is the bifurcation boundary shown in Figure 4.

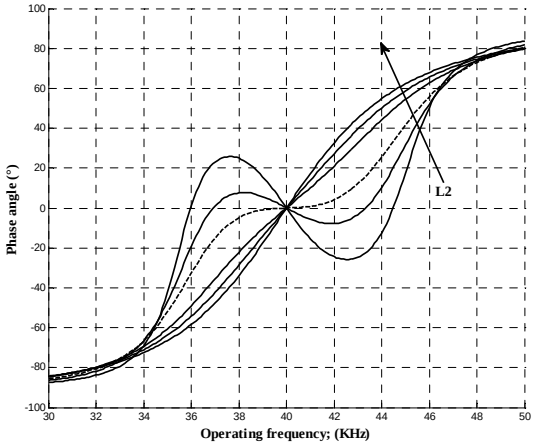

Figure 4. Bifurcation phenomenon with varied secondary inductance.

If L_2 is higher than k_a , it can be seen that the zero phase angle frequency is unique and equal to the secondary resonant frequency. If L_2 is lower than k_a , there are three zero phase angle frequency points and the bifurcation occurs.

B. Constrained inequality based on components peak over-voltage and peak withstand current

To achieve the required performance, each component must function properly through the operation period. The components of the system should be operated under the peak over-voltage and peak withstand current. Under these conditions, four nonlinear constrained inequalities can be obtained, as shown in:

$$\begin{cases} I_1(L_1, L_2) < I_{s1} \\ V_1(L_1, L_2) < V_{s1} \\ I_2(L_1, L_2) < I_{s2} \\ V_2(L_1, L_2) < V_{s2} \end{cases} \tag{11}$$

where $I_1(L_1, L_2)$, $V_1(L_1, L_2)$, $I_2(L_1, L_2)$ and $V_2(L_1, L_2)$ are the functions of the primary current, primary compensation capacitance voltage, secondary current and secondary compensation capacitance voltage, respectively. I_{s1} , I_{s2} , V_{s1} and V_{s2} denote peak withstand currents and the peak compensation

capacitance over-voltages in the primary and secondary circuits respectively.

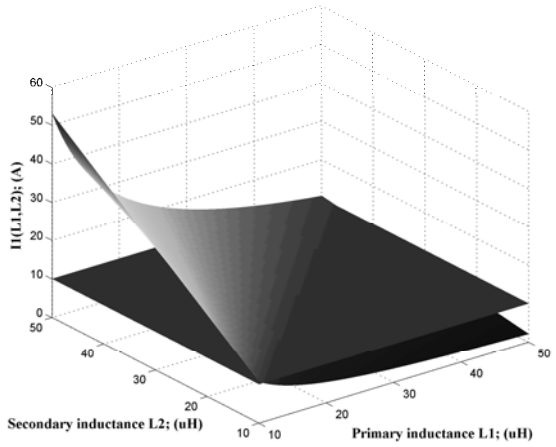

(a) $I_1(L_1, L_2)$ versus I_{s1}

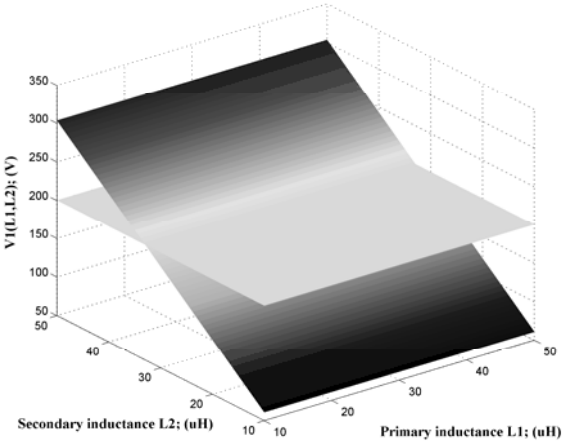

(b) $V_1(L_1, L_2)$ versus V_{s1}

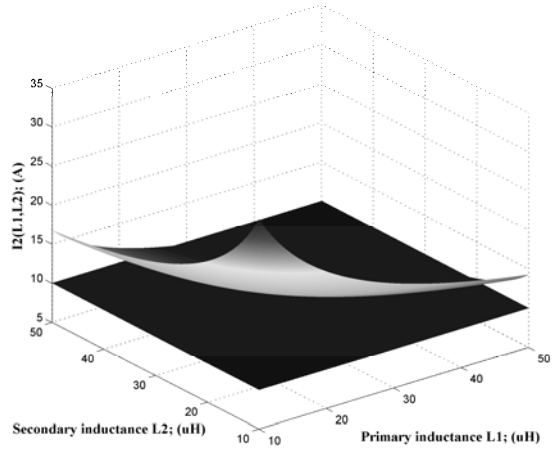

(c) $I_2(L_1, L_2)$ versus I_{s2}

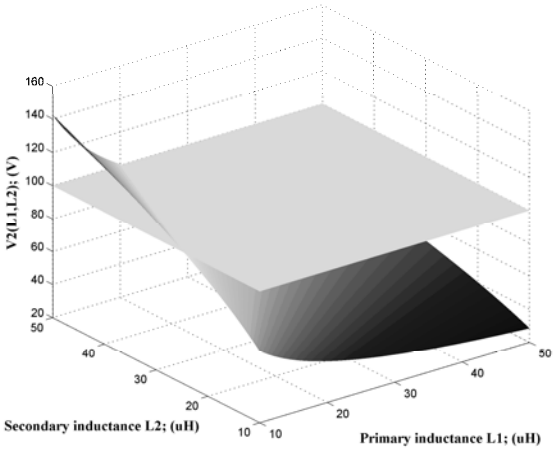

(d) $V_2(L_1, L_2)$ versus V_{s2}

Figure 5. Constrained conditions variation with primary and secondary inductance.

In Figure 5, the constrained conditions based on inequality (11) variation with primary and secondary inductance is shown. It is seen from Figure 5, the functions should be chosen below the plane. I_{s1}, I_{s2}, V_{s1} and V_{s2} are set to be 10A, 200V, 10A and 100V respectively, which are based on the system behaviors.

From Figure 3, when L_1=10 μH, L_2=50 μH, the system achieving maximum power transfer capability 500W. But from Figure 5 it is seen that, this optimum value can not achieved because of constrains proposed before. Thus, the optimization model is employed, and an iterative calculation must be performed, which can be easily implemented using MATLAB Optimization Toolbox.

In the MATLAB Optimization Toolbox, most of these optimization routines require the objective function to be minimized. So the maximization is achieved by supplying the routines with $-P_2(L_1, L_2)$, where $P_2(L_1, L_2)$ is the function being optimized.

Taken together, the optimization model based on this study can be described as follows:

$$\begin{aligned} &\textit{Minimize} && -P_2(L_1, L_2) \\ &\textit{Subject To} && \mathrm{g}(L_1, L_2) = \begin{cases} I_1(L_1, L_2) < I_{s1} \\ V_1(L_1, L_2) < V_{s1} \\ I_2(L_1, L_2) < I_{s2} \\ V_2(L_1, L_2) < V_{s2} \\ k_a < L_2 \end{cases} \end{aligned} \tag{12}$$

TABLE Ⅱ The solutions of algorithm

Specification	Optimization Results
L_1 (μH)	45.11
L_2 (μH)	27.21
C_1 (μF)	0.37
C_2 (μF)	0.58

An interior point algorithm is employed to search for maximum value of objective. The results of optimization

are listed in TABLE II, C_1 and C_2 are calculated by equation (5) and (6).

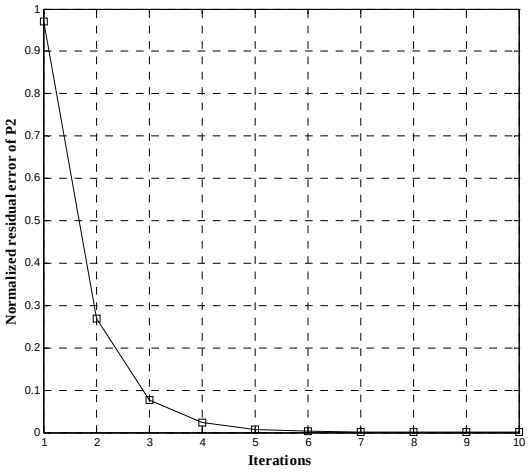

Figure 6. Normalized residual error of P_2 versus iterations.

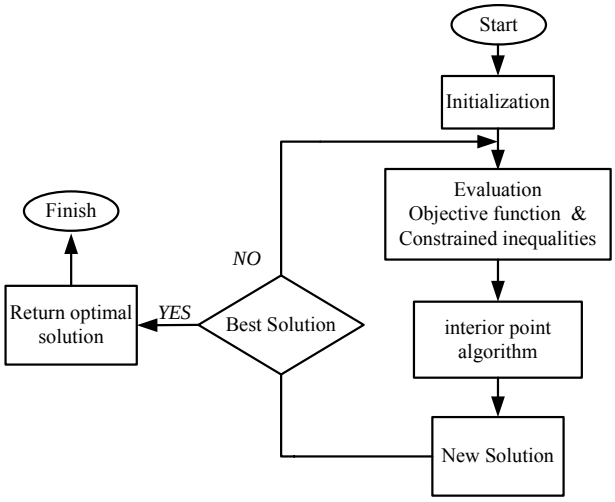

Figure 7. Optimization flowchart.

Figure 6 shows the performance of this optimization algorithm. The plots show the relative decrease in the normalized residual error versus the iterations. From Figure 6 it is seen that, within 10 iterations, algorithm achieved their maximum values. Figure 7 shows the flowchart of the optimization.

IV. SIMULATED AND EXPERIMENTAL VERIFICATION

In order to verify the proposed optimization model as well as testify its accuracy, the calculated results are compared with the results obtained from both MATLAB/SIMULINK simulation and experimental tests.

The TET system shown in Figure 2 has been simulated with SIMULINK software package. The input DC voltage $V_{dc} = 15V$, $R_L = 20\Omega$, $f = 40kHz$, $L_1 = 45.11\mu H$, $L_2 = 27.21\mu H$, $M = 8.41\mu H$, $C_1 = 0.37\mu F$, $C_2 = 0.58\mu F$, $k = 0.24$.

Figure 8 shows the simulated H-bridge output voltage waveforms and secondary output voltage waveforms when L_1 and L_2 are set to optimal value which is shown in TABLE II.

Figure 8(a) is H-bridge output voltage and (b) is secondary output voltage. From simulated results, it is seen from Figure 8 (b), the peak value of the output voltage is 53.10V and the RMS value is 37.55V. The load resistance is 20Ω, so the output power is 70.50W.

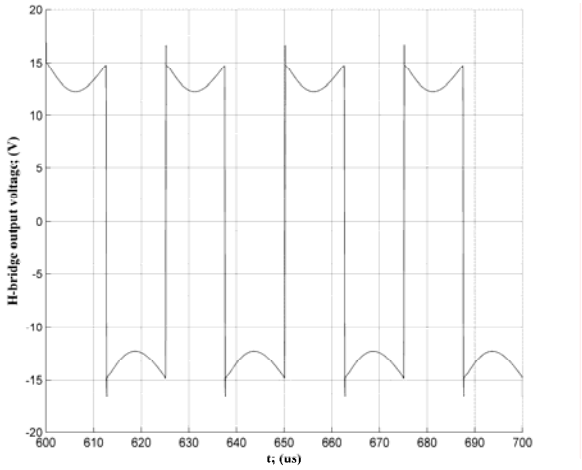

(a) H-bridge output voltage

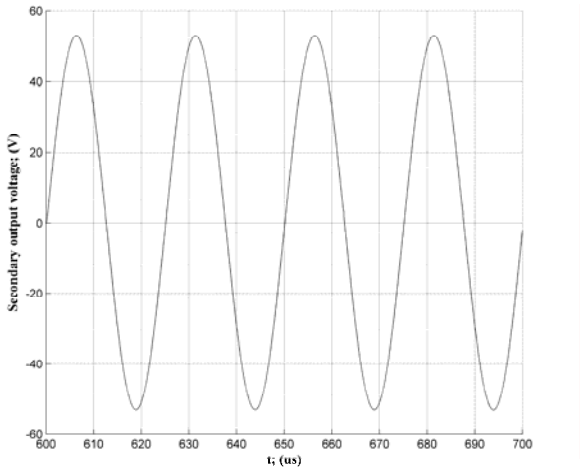

(b) Secondary output voltage

Figure 8. Simulated results of the H-bridge output voltage and secondary output voltage.

To further demonstrate the effectiveness of the new method, a prototype of the TET system was implemented. An experimental circuit has been set up for verification using the same circuit parameters. Figure 9 shows the experimental H-bridge output voltage waveforms and secondary output voltage waveforms when L_1 and L_2 are set to optimal value. Figure 9(a) is H-bridge output voltage and (b) is secondary output voltage. Comparing Figure 8 with Figure 9, there is very good agreement between the measured and simulated power transfer. So the optimization model is validated to design the TET system.

From experimental results, shown in Figure 9 (b), the peak value of the output voltage is 45.60V and the RMS value is 32.24V. The load resistance is 20Ω, so the output power is 51.97W.

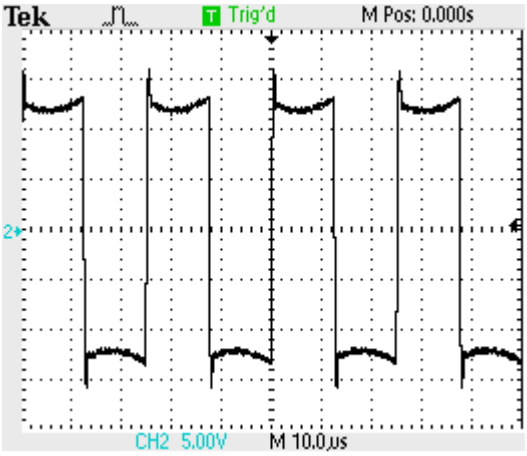

(a) H-bridge output voltage. (5V/division)

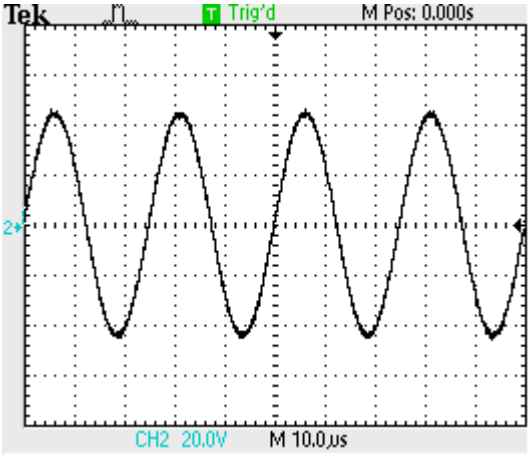

(b) Secondary output voltage. (20V/division)

Figure 9. Experimental results of the H-bridge output voltage and secondary output voltage.

Although the shapes of experimental and simulated curve are in good agreement, the experimental output power deviates by about 18W. This is caused by neglect the internal resistance in simulation model, and it is difficult to get exactly the required capacitance and inductance.

Figure 10 (a) shows the output power of the TET system when inductance L_1 increases and inductance L_2 is set to its optimal value. It is shown that when L_1 is increased; the output power is lower than the design value.

Figure 10 (b) shows the primary and secondary current of the TET system when inductance L_1 varies and inductance L_2 is set to its optimal value. It is shown that when L_1 is decreased; although the calculated output power is greater than optimal value, the primary current exceed primary peak withstand current $I_{s1} = 10A$ (shown in section III), may lead to the damage and breakdown of the TET system.

The output power when inductance L_2 varies and inductance L_1 is tuned to its optimal value is shown in Figure 10 (c). It is shown that when L_2 is decreased; the output power is lower than the design value.

Figure 10 (d) shows the primary and secondary current of the TET system when inductance L_2 varies and inductance L_1 is set to its optimal value. It is shown that when L_2 is increased; although the calculated output power is greater than optimal value, the primary current exceed primary peak withstand current $I_{s1} = 10A$ (shown in section III), may lead to the damage and breakdown of the TET system.

Therefore, in steady-state, the maximum value of the output power is achieved when primary and secondary inductances are set to optimal value.

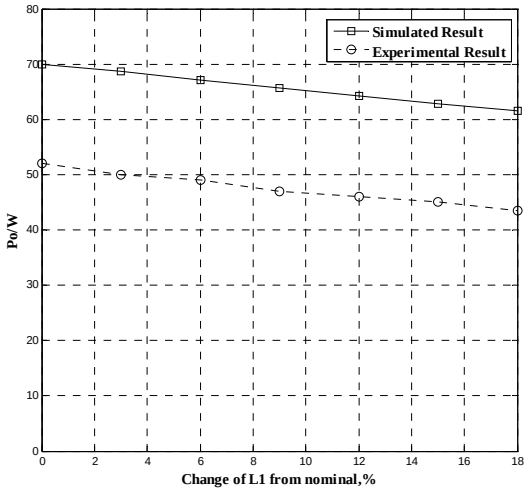

(a) Output power against change in primary inductance value

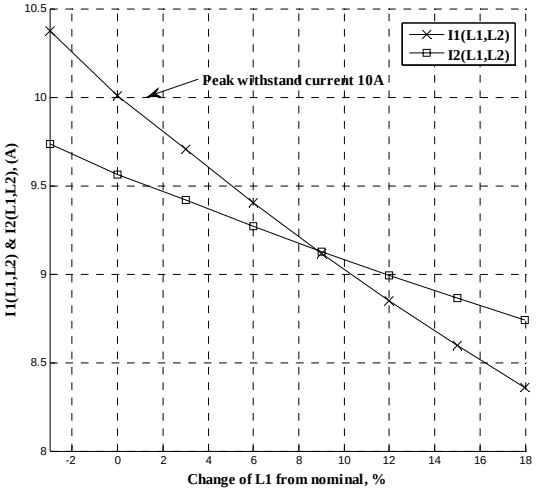

(b) Primary and secondary current against change in primary inductance value

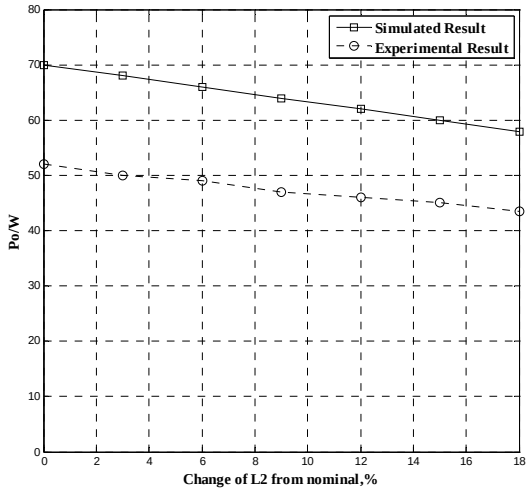

(c) Output power against change in secondary inductance value

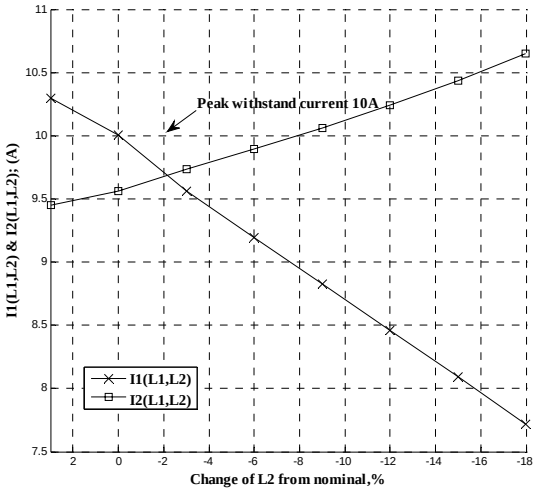

(d) Primary and secondary current against change in secondary inductance value

Figure 10. Output power, primary current and secondary current against change in inductance value.

V. CONCLUSIONS

TET system is well known, but in practice it is difficult to determine the parameters of the coils. In this paper, an optimization model for the coil inductance calculation has been established and verified. Theoretical design is verified by simulation model and experimental results. There is very good agreement between the simulated result and experimental result.

The proposed optimization model can be used to easily and quickly determine the value of two coils. This new optimization model provides a new and useful tool for preliminary system design.

REFERENCES

[1] Halperin, D., Kohno, T., Heydt-Benjamin, T. S., Fu, K. and Maisel, W. H. "Security and privacy for implantable medical devices," *IEEE Pervas. Comput.*, vol. 7, no. 1, pp. 30-39, 2008.

[2] Schuder, J. C. "Powering an artificial heart: birth of the inductively coupled-radio frequency system in 1960," *Artif. Organs.*, vol. 26, no. 11, pp. 909-915, November 2002.

[3] P. Zan, G. Yan, H.Liu, N. Luo and Y. Zhao, "Adaptive transcutaneous power delivery for an artificial anal sphincter system" Journal of Medical Engineering & Technology, vol. 33, pp136–141, 2009.

[4] Qianhong Chen, Siu Chung Wong and Tse, C. K. "Analysis, design, and control of a transcutaneous power regulator for artificial hearts," *IEEE Trans. Biomed. Circuits Syst.*, vol. 3, no. 1, pp. 23–31, February 2009.

[5] Wu, H. H., Hu, A. P., Malpas, S.C. and Budgett,D.M. "Determining optimal tuning capacitor values of TET system for achieving maximum power transfer," *Electron. Lett.*, vol. 45, no. 9, pp. 448-449, April 2009.

[6] Arai, S., Miura, H., Sato, F., Matsuki, H. and Sato, T. "Examination of circuit parameters for stable high efficiency TETS for artificial hearts," *IEEE Trans. Magn.*, vol. 41, no. 10, pp. 4170-4172, October 2005.

[7] Valtchev, S., Borges, B., Brandisky, K. and Klaassens, J. B. "Resonant contactless energy transfer with improved efficiency," *IEEE Trans. Power Electron.*, vol.24, no. 3, pp. 685-699, March 2009.

[8] Dissanayake, T. D., Hu, A. P., Malpas, S., Bennet, L., Taberner, A., Booth, L. and Budgett, D. "Experimental study of a TET system for implantable biomedical devices," *IEEE Trans. Biomed. Circuits Syst.*, vol. 3, no. 6, pp. 370-378, December 2009.

[9] Chwei-Sen Wang, Covic, G. A., Stielau, O. H. "Power transfer capability and bifurcation phenomena of loosely coupled inductive power transfer systems," *IEEE Trans. Ind. Electron.*, vol. 51, no. 1, pp. 148-156, February 2004.

[10] Chwei-Sen Wang, Stielau, O. H. and Covic, G. A. "Design considerations for a contactless electric vehicle battery charger," *IEEE Trans. Ind. Electron.*, vol. 52, no. 5, pp. 1308-1314, October 2005.

[11] Hu, A.P. "Modeling a contactless power supply using GSSA method," *IEEE International Conference on Industrial Technology*, February 2009.

[12] Liu, W. Tang, H. J., Fang, W. and Ye, P. S. "Estimation of the non-measurable state variables of a transcutaneous energy transmission system for artificial human implants using extended Kalman filters," *Circuits Syst. Signal Process.*, vol. 28, no. 4, pp. 581-593, March 2009.

[13] W. Fang, W. Liu, J. Qian, H. J. Tang, and P. S. Ye, "Modeling and Simulation of a Transcutaneous Energy Transmission System Used in Artificial Organ Implants," *Artificial Organs,* vol. 33, pp. 1069-1074, Dec 2009.

[14] W. Fang, H. J. Tang, and W. Liu, "Modeling and analyzing an inductive contactless power transfer system for artificial hearts using the generalized state space averaging method," *Journal of Computational and Theoretical Nanoscience,* vol. 4, pp. 1412-1416, Nov-Dec 2007.

[15] Chwei-Sen, Wang, Covic, G. A. and Stielau, O. H. "Investigating an LCL load resonant inverter for inductive power transfer applications," *IEEE Trans. Power Electron.*, vol. 19, no. 4, pp. 995-1002, July 2004.

[16] C. M. Zierhofer and E. S. Hochmair "Geometric approach for coupling enhancement of Magnetically coupled coils," *IEEE Trans. Biomed. Eng.*, vol. 43, no. 7, pp. 708-714, July 1996.

[17] Ping Si, Hu, A. P., Malpas, S., and Budgett, D. "A frequency control method for regulating wireless pwer to implantable devices," *IEEE Trans. Biomed. Circuit Syst.,* vol. 2, no. 1, pp. 22-29, March 2008.

[18] Jesús Sallán, Juan L. Villa, Andrés Llombart, and José Fco. Sanz, "Optimal design of ICPT system applied to electric vehicle battery charge," *IEEE Trans. Ind. Electron.*, vol. 56, no. 6, pp. 2140-2149, June 2009.
[19] Xun Liu and Hui, S. Y., "Optimal design of a hybrid winding struture for planar contactless battery charging platform," *IEEE Trans. Power Electron.*, vol. 23, no. 1, pp. 455-463, January 2008.
[20] E. Okamoto, Y. Yamamoto, Y. Akasaka, T. Motomura, Y. Mitamura, and Y.Nose, "A New Transcutaneous Energy Transmission System With Hybrid Energy Coils for Driving an Implantable Biventricular Assist Device," *Artif. Organs.*, vol. 33, pp. 622-626, August 2009.

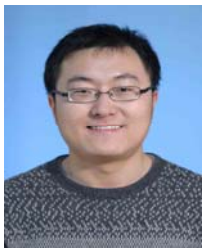

Liangyu Bai was born in Shanxi province, China, in 1983. He received the B.S. degree in electrical engineering from Yanshan University, Qinhuangdao, China, in 2004, and M.S. degree in electrical engineering from Guangxi University, Nanning, in 2008. He is currently working toward his Ph.D. degree in electrical engineering at Shanghai Jiao Tong University.

His research interests include power electronics and wireless power transfer.

Houjun Tang was born in Shandong province, China, in 1957. He received B.S. and M.S. degrees in 1982 and 1988 respectively. He received Ph.D. degree in Yamagata University, Japan, 1997. He is Professor of the Department of Electrical Engineering, Shanghai Jiao Tong University.

His current research interests include automotive electronics, wireless power transfer.

Yang Xu was born in Hubei province, China, in 1984. He received the B.S. and M.S. degree in electrical engineering from Jiangsu University of Science and Technology, Zhenjiang, China, in 2006, 2009. He is currently working toward the Ph.D. degree in electrical engineering from Shanghai Jiao Tong University.

His research interests include power electronics and wireless power transfer.